

EQUILIBRIUM CONFIGURATIONS FOR A TERRITORIAL MODEL *

RONALD VOTEL[†], DAVID A. W. BARTON[‡], AND JEFF MOEHLIS[§]

Abstract.

We consider a territorial model based on Voronoi tessellations. Such tessellations form a partitioning of a planar region by enclosing each agent in a polygon such that every point within the polygon is closest to that agent instead of any other. For rectangular domains and for small population sizes, we show that there can be distinct coexisting stable equilibrium configurations, including the possibility of stable equilibria that are not related by symmetry. By considering randomly distributed initial positions, we give a statistical characterization of the basins of attraction for these equilibria in the case of a square domain. Furthermore, we show that the final territory that an agent occupies can have a wide range of sizes, which suggests that an individual can obtain a competitive advantage or disadvantage due entirely to its initial position. Finally, by treating the ratio of the length of the shorter side to the length of the longer side of the rectangle as a bifurcation parameter, we numerically explore how stable and unstable equilibrium configurations are related to each other.

Key words. territorial behavior, Voronoi tessellations, symmetry

AMS subject classifications.

1. Introduction. One of the most fundamental problems in all of biology is to understand how organisms divide space into discrete territories that define their abilities to capture vital resources and access mates. A *territory* is a geographical area that an individual animal consistently defends against other individuals from its own species, typically in an attempt to maximize its reproductive opportunities and/or to secure food resources for itself and its young [28]. Territoriality is common across nearly all major groups of organisms on the planet. While higher animals like vertebrates exhibit the most obvious territorial boundaries, lower animals like invertebrates, plants, fungi and possibly even bacteria are known to aggressively defend space through behaviors and chemicals.

We highlight the experiment in [2], which involved placing a number of mouth-breeder fish *Tilapia mossambica* in a rectangular pool with a sandy floor. The males vying for suitable breeding territory dug pits, spitting sand away from their pit centers. The resulting rims of the pits were visualized in a top-view photograph taken with a polarizing filter, which showed that the final arrangement of pits resembled a honeycomb-like pattern consisting mainly of pentagonal and hexagonal regions. It has been shown [21, 27] that these territories can be approximated by Voronoi tessellations [15], a partition of the (top-view projection of the) pool formed by enclosing each fish in a polygon such that every point within the polygon is closest to that particular fish instead of any other. Other observational determinations of territorial boundaries include [18, 3, 4, 5, 14].

*This work was supported by National Science Foundation grant NSF-0434328, an Alfred P. Sloan Research Fellowship in Mathematics (JM), and a Lloyds Tercentenary Foundation Fellowship (DAWB). We thank Brad Cardinale for useful discussions related to this research.

[†]Department of Aeronautics and Astronautics, School of Engineering, Stanford University, Stanford, CA 94305-4035, United States of America (rvotel@stanford.edu)

[‡]Department of Engineering Mathematics, Queen's Building, University Walk, University of Bristol, Bristol, BS8 1TR, United Kingdom (david.barton@bristol.ac.uk)

[§]Department of Mechanical Engineering, University of California, Santa Barbara, CA 93106, United States of America (moehlis@engineering.ucsb.edu)

Various mathematical models have been developed to understand sizes and shapes that territories will take for different species of animals. Some models determine the optimal size for an agent’s territory based on a function which balances benefits of having a larger territory with the costs of defending such a territory; see [1] and references therein. In this paper, we instead consider the dynamical model, based on Voronoi tessellations, which was studied in [27]; also see [19, 20]. In particular, the agents move toward the centroid of their current Voronoi cell, continuing such adjustment until an equilibrium state is reached. This model captures the tendency of each agent to occupy territory so that it is as far from others as possible, and the notion that aggression of an agent decreases monotonically with distance from the center of its territory. We ignore environmental influences and heterogeneity in the individuals’ characteristics or behavior, and assume that the settlement is synchronous, i.e., all agents begin competing for territory at the same time. The simulations in [27] of this model focused on the behavior of large numbers of agents ($N = 500$) for periodic boundary conditions, and showed good agreement between the statistics of the territorial shapes from the model and those found for the experiment in [2]. We note that other “territorial” models involving Voronoi tessellations have been studied in the robotics literature, e.g. [9, 23].

In Section 2 we describe the model from [27] in more detail. In Section 3 we consider the model for a small population ($N = 2$ up to $N = 9$) in a square domain for which the boundaries of the domain form boundaries of the Voronoi cells, as appropriate. We find that for certain population sizes there are distinct coexisting stable equilibrium configurations, sometimes related by symmetry and sometimes not. We give a statistical characterization of the likelihood of the system reaching different equilibria, and show that an agent can end up with a much larger or smaller territory (and corresponding competitive advantage or disadvantage) than other agents. In Section 4, we consider the model for a small population in a rectangular domain, again with the boundaries of the domain forming boundaries of the Voronoi cells as appropriate. By treating L , the ratio of the length of the shorter side to the length of the longer side of the rectangle, as a bifurcation parameter, we numerically explore how stable and unstable equilibrium configurations are related to each other, and identify rectangles which have coexisting stable equilibrium configurations. Concluding remarks are given in Section 5. We focus on small numbers of agents and square and rectangular domain shapes because these are natural for controlled laboratory experimentation which could test the validity of the model.

2. The Model . We consider N agents in a two-dimensional rectangular domain D with sides of length 1 and L . Without loss of generality, we take $L \leq 1$, where equality corresponds to the special case of a square domain. The location of the i^{th} agent at time step n is $\mathbf{x}_i^{(n)}$. The Voronoi cell [15] for the i^{th} agent at time step n is defined as

$$V_i^{(n)} = \{\mathbf{x} \in D \mid |\mathbf{x} - \mathbf{x}_i| < |\mathbf{x} - \mathbf{x}_j| \quad \text{for } j = 1, \dots, N, j \neq i\}, \quad (2.1)$$

with centroid

$$\mathbf{c}_i^{(n)} = \frac{1}{|V_i^{(n)}|} \int_{V_i^{(n)}} \mathbf{x} d\mathbf{x}, \quad (2.2)$$

where $|V_i^{(n)}|$ is the area of Voronoi cell $V_i^{(n)}$. Each agent's location at time step $n + 1$ is determined as [27]

$$\mathbf{x}_i^{(n+1)} = \mathbf{x}_i^{(n)} + (\mathbf{c}_i^{(n)} - \mathbf{x}_i^{(n)})/M, \quad i = 1, \dots, N, \quad (2.3)$$

where M is a constant greater than or equal to 1; that is, each agent moves a fraction of the distance toward the centroid of its Voronoi cell.

We simulate this model using Matlab, taking advantage of its built-in `voronoi` and `voronoin` commands, and using John Burkhardt's publicly available Matlab geometry command package to perform certain calculations such as finding centroids of the Voronoi cells from their vertices [7]. To force the boundaries of Voronoi cells to be the boundaries of D , as appropriate, we place four images of each agent outside D (one reflected about each side of D) for each agent.

Numerical simulation reveals that for all cases considered ($N = 2, \dots, 9$, various values of M , and many random and non-random initial conditions) the dynamical system (2.3) equilibrates as $n \rightarrow \infty$ to a stable equilibrium configuration satisfying

$$\mathbf{x}_i^{(n+1)} = \mathbf{x}_i^{(n)}, \quad i = 1, \dots, N. \quad (2.4)$$

Stability may be confirmed numerically by calculating the eigenvalues (using finite differences) of the linearization of the system about the equilibrium configuration. We find that for certain values of N and L , there are distinct coexisting stable equilibrium configurations, sometimes related by symmetry and sometimes not. For this model, we do not find more complicated attractors such as periodic orbits.

3. Results for Square Container .

3.1. Symmetry Considerations. Before giving details of the stable equilibrium configurations, it is helpful to clarify the symmetry aspects of this system by using a treatment based on [16, 8, 17, 22, 26]. (Also see [25] for a nice introduction to group theory.) When D is a square, the evolution equations (2.3) are equivariant with respect to the eight element group D_4 , which is generated by a 90° rotation R (which we take to be counterclockwise) and a diagonal reflection d (which we take to be about the line from the lower left to the upper right corner of D). This implies that if X is an equilibrium configuration, then so is every configuration on its group orbit, that is, the set of configurations $\gamma \cdot X$ for all $\gamma \in D_4$, which we denote by $D_4 \cdot X$. The symmetry of an equilibrium configuration X is characterized by its isotropy subgroup

$$\Sigma_X = \{\gamma \in D_4 : \gamma \cdot X = X\}, \quad (3.1)$$

that is, the set of all elements of D_4 which leave X unchanged. In determining the isotropy subgroup and the group orbit, we only consider the shape of the boundaries of the Voronoi cells, and in particular do not consider the "labels" for the agents. (This is equivalent to associating all configurations related by the permutation symmetry which relabels agents.) From Proposition 1.2 of [16], we expect that

$$8 = |D_4| = |\Sigma_X| |D_4 \cdot X|, \quad (3.2)$$

that is, the number of elements of the group D_4 (namely, 8) equals the product of the size of the isotropy subgroup of X times the number of (distinct) elements in the

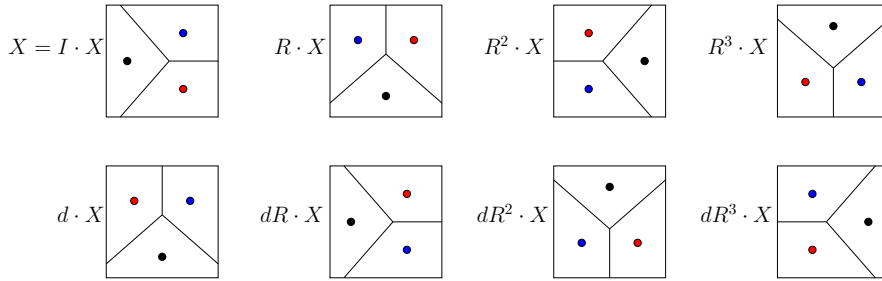


FIG. 3.1. Sketches of possible stable equilibrium configurations for $N = 3$ agents for a square domain, obtained through the actions of the elements of D_4 on the configuration X . R gives a counterclockwise rotation through 90° , and d gives a reflection about the diagonal from the lower left to the upper right corners of the square. The color of the agents enables them to be uniquely identified after each group operation. However, in determining the isotropy subgroup of such configurations, we only consider the shapes of boundaries of the Voronoi cells, indicated by lines, and not permutations of the individual agents. We see that this example configuration X has an isotropy subgroup $\Sigma_X = \{I, dR\}$. Furthermore, the group orbit (only indicating distinct configurations based on the boundaries of the Voronoi cells) can be taken to be the set of configurations $\{X, R \cdot X, R^2 \cdot X, R^3 \cdot X\}$.

group orbit of X . Finally, we note that the isotropy subgroups of X and $\gamma \cdot X$ are related by the conjugacy [16]

$$\Sigma_{\gamma \cdot X} = \gamma \Sigma_X \gamma^{-1}. \quad (3.3)$$

We will use the convention that the order of group element operation is from right to left. For example, in determining the effect of dR on a configuration X (i.e., $dR \cdot X$), we first rotate (R), then reflect (d). Furthermore, we denote the identity group operation, which leaves the configuration unchanged, by I .

We now illustrate these symmetry ideas for the stable equilibrium configurations found for $N = 3$. Figure 3.1 shows a configuration X and its group orbit under D_4 . Remembering that we only consider the shape of the boundaries of the Voronoi cells in determining the isotropy subgroup, we see that

$$\Sigma_X = \{I, dR\}, \quad (3.4)$$

and that the group orbit of X can be taken to be the set of configurations

$$\{X, R \cdot X, R^2 \cdot X, R^3 \cdot X\}. \quad (3.5)$$

This is consistent with (3.2). Figure 3.2 shows the group orbit of the configuration $Y = R \cdot X$. We see that its isotropy subgroup is

$$\Sigma_Y = \{I, dR^3\}. \quad (3.6)$$

Now,

$$R \cdot \Sigma_X \cdot R^{-1} = R \cdot \{I, dR\} \cdot R^{-1} = \{I, dR^3\} = \Sigma_{R \cdot X} = \Sigma_Y, \quad (3.7)$$

as expected from (3.3).

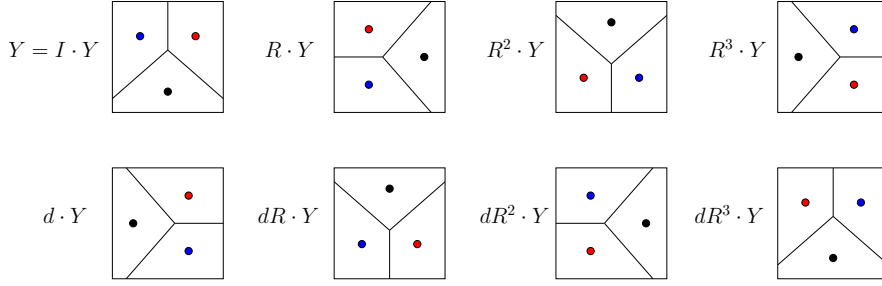


FIG. 3.2. Sketches of possible stable equilibrium configurations for $N = 3$ agents for a square domain obtained through the actions of the elements of D_4 on the configuration $Y = R \cdot X$. Configuration Y thus has isotropy subgroup $\Sigma_Y = \{I, dR^3\}$. Furthermore, the group orbit can be taken to be the set of configurations $\{Y, R \cdot Y, R^2 \cdot Y, R^3 \cdot Y\}$.

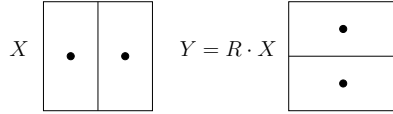


FIG. 3.3. Stable equilibrium configurations for $N = 2$ agents for a square domain. These configurations are related by symmetry, and have the same isotropy subgroup. Recall that we associate configurations related by the permutation symmetry which relabels agents.

Configurations related by symmetry do not necessarily have different isotropy subgroups. For example, the configurations X and $Y = R \cdot X$ in Figure 3.3 both have isotropy subgroup

$$\Sigma_X = \Sigma_Y = \{I, R^2, dR, dR^3\}.$$

Note that it is readily shown that $R \cdot \Sigma_X \cdot R^{-1} = \Sigma_X$.

3.2. Equilibrium Configurations. Figure 3.4 shows one representative from each distinct set of symmetry-related stable equilibria for $N = 2, \dots, 9$. We find that for $N = 5, 6, 7$, and 9 , coexisting stable equilibria which are *not* related by symmetry occur. (Note that for rectangular domains, coexisting stable equilibria not related by symmetry also exist for $N = 3$ and $N = 4$, as described in Section 4.) Table 3.1 shows the probability of reaching a stable equilibrium configuration of each type with random initial positions distributed uniformly on D for $N = 2, \dots, 9$ and several values of M . For example, for $N = 5$ and $M = 1$, there is an 88.5% chance of asymptotically approaching one of the elements of the group orbit of the equilibrium configuration Va shown in Figure 3.4. (Our numerics confirm the expected result that there is an equal probability of reaching each of the equilibria on a group orbit.) This table thus gives a statistical characterization of the relative sizes of the basins of attraction for the various stable equilibrium configurations. We see that the probability of reaching a particular equilibrium depends only weakly on M .

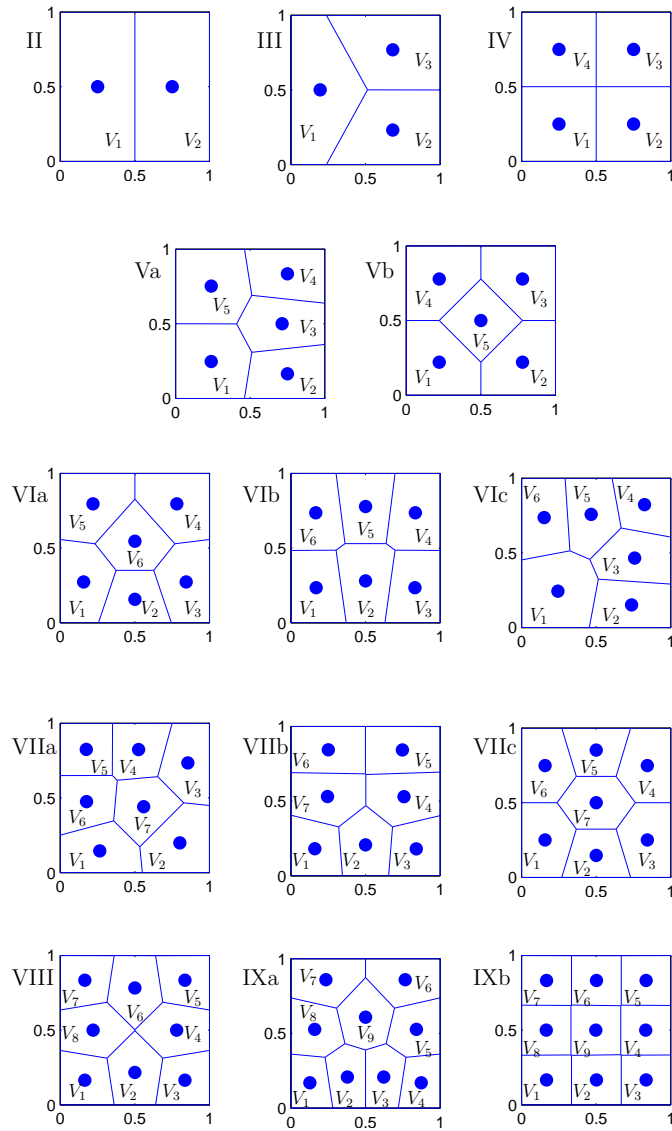


FIG. 3.4. Stable equilibrium configurations found numerically for $N = 2, \dots, 9$ for a square domain. Symmetry-related equilibria (i.e., other elements on the group orbit of an equilibrium) are not shown. The equilibria are labeled with a roman numeral indicating the value of N , and a lower-case letter to distinguish different equilibria for a given N , if necessary. The index i in the cell label V_i is only for reporting the areas in Table 3.2; recall that we associate all configurations related by the permutation symmetry which relabels agents.

equil	isotropy	$M = 1$	$M = 4$	$M = 8$	$M = 12$	$M = 16$	$M = 20$
II	$\{I, R^2, dR, dR^3\}$	100	100	100	100	100	100
III	$\{I, dR\}$	100	100	100	100	100	100
IV	D_4	100	100	100	100	100	100
Va	$\{I, dR\}$	88.5	87.5	89	85.5	86	86.5
Vb	D_4	11.5	12.5	11	14.5	14	13.5
VIa	$\{I, dR^3\}$	49	49	54	42	42	40.5
VIb	$\{I, dR^3\}$	22.5	22.5	14	21.5	22	19.5
VIc	$\{I, d\}$	28.5	28.5	32	36.5	36	40
VIIa	$\{I, dR^2\}$	49	50	37.5	42.5	44.5	47
VIIb	$\{I, dR^3\}$	25.5	28.5	35.5	32	27.5	32.5
VIIc	$\{I, R^2, dR, dR^3\}$	25.5	21.5	27	25.5	28	20.5
VIII	D_4	100	100	100	100	100	100
IXa	$\{I, dR^3\}$	12.5	9.5	10	14	16	15.5
IXb	D_4	87.5	90.5	90	86	84	84.5

TABLE 3.1

For the equilibrium configurations for a square domain as labeled in Figure 3.4, we give the isotropy subgroup and probability of reaching one of the equilibria on its group orbit for random initial positions distributed uniformly on D and different values of M . The probabilities were calculated from 200 random initial positions for each value of N .

Table 3.2 gives the areas of the different cells for the configurations shown in Figure 3.4. We notice that these areas can differ widely for certain N values. For example, when $N = 5$ an agent in cell V_1 (or V_5) for configuration Va occupies 23.8% of the available territory, while an agent in cell V_5 for configuration Vb only occupies 15.6%. More substantially, when $N = 6$ an agent in cell V_1 for configuration VIc occupies 23.3% of the available territory, while an agent in cell V_4 for the same configuration, or an agent in cell V_2 for configuration VIa, only occupies approximately 13%. This suggests that an individual can have a major competitive advantage or disadvantage based on territorial size due entirely to the initial positions of the agents, as this determines the configuration which the population equilibrates to and the cell in which each agent ends up.

There are also various unstable configurations for a square domain that cannot be found by numerical simulation alone, as will be shown in the next section.

4. Results for Rectangular Container .

4.1. Symmetry Considerations. When D is a (non-square) rectangle, the evolution equations (2.3) are equivariant with respect to the four element group

$$D_2 = \{I, R^2, dR, dR^3\}$$

which is a subgroup of the group D_4 discussed in Section 3. The elements R^2 , dR , and dR^3 correspond to a rotation by 180° , reflection about the horizontal midplane, and reflection about the vertical midplane, respectively. The possible isotropy subgroups of equilibrium configurations for a rectangular container are D_2 , $\{I, R^2\} \cong Z_2$, $\{I, dR\} \cong Z_2$, $\{I, dR^3\} \cong Z_2$, and $\{I\}$. As in Section 3, in determining the isotropy subgroup of a configuration we only consider the shape of the boundaries of the Voronoi cells.

equil	areas		
II	$ V_1 = V_2 = 0.5$		
III	$ V_1 = 0.376$	$ V_2 = 0.312$	$ V_3 = 0.312$
IV	$ V_1 = V_2 = V_3 = V_4 = 0.25$		
Va	$ V_1 = V_5 = 0.238$	$ V_2 = V_4 = 0.172$	$ V_3 = 0.181$
Vb	$ V_1 = V_2 = V_3 = V_4 = 0.211$		$ V_5 = 0.156$
VIa	$ V_1 = V_3 = 0.168$	$ V_2 = 0.130$	$ V_4 = V_5 = 0.192$
VIb	$ V_1 = V_3 = 0.163$	$ V_2 = 0.174$	$ V_4 = V_6 = 0.171$
VIc	$ V_1 = 0.233$	$ V_2 = V_6 = 0.159$	$ V_3 = V_5 = 0.158$
VIIa	$ V_1 = V_3 = 0.154$	$ V_2 = 0.172$	$ V_4 = V_6 = 0.129$
VIIb	$ V_1 = V_3 = 0.121$	$ V_2 = 0.135$	$ V_4 = V_7 = 0.154$
VIIc	$ V_1 = V_3 = V_4 = V_6 = 0.156$		$ V_2 = V_5 = 0.118$
VIII	$ V_1 = V_3 = V_5 = V_7 = 0.113$		$ V_2 = V_4 = V_6 = V_8 = 0.136$
IXa	$ V_1 = V_4 = 0.089$	$ V_2 = V_3 = 0.099$	$ V_5 = V_8 = 0.114$
IXb	$ V_1 = V_2 = V_3 = V_4 = V_5 = V_6 = V_7 = V_8 = V_9 = 0.111$		$ V_6 = V_7 = 0.134$

TABLE 3.2

For the equilibrium configurations for a square domain as labeled in Figure 3.4, we give the area $|V_i|$ for each Voronoi cell V_i .

4.2. Bifurcation Analysis. We treat L , the ratio of the length of the shorter side to the length of the longer side of the rectangle, as a bifurcation parameter. Without loss of generality, we take $L \leq 1$, where equality corresponds to the special, degenerate case of a square domain. Note that the bifurcation results are independent of M , which determines the fraction of the distance an agents moves toward the centroid of its Voronoi cell.

In order to determine how the equilibrium configurations change as L is varied, we use the method of numerical continuation. Various software packages exist for numerical continuation of differential equations and maps, such as AUTO [13] and MatCont [10]. These packages use the method of pseudo-arclength continuation in a predictor-corrector manner which enables both stable and unstable solutions to be found [11, 12]. A predicted solution is extrapolated from one or more known solutions and then corrected, using a nonlinear solver, to be a solution of the dynamical system with constraints provided by the pseudo-arclength conditions. The sequence of corrected solutions that is produced can be viewed as a discretized solution branch in the appropriate system parameters. Bifurcations, detected using suitable test functions, and the corresponding bifurcating solution branches can also be continued.

We continue equilibrium configurations of the evolution equations (2.3) using the authors' own software package written entirely in Matlab to enable the built-in `voronoi` and `voronoin` commands to be used. This package, built around Matlab's nonlinear solver (`fsolve`), uses the same numerical algorithms as described above for AUTO and MatCont. Bifurcation detection is performed by monitoring the eigen-

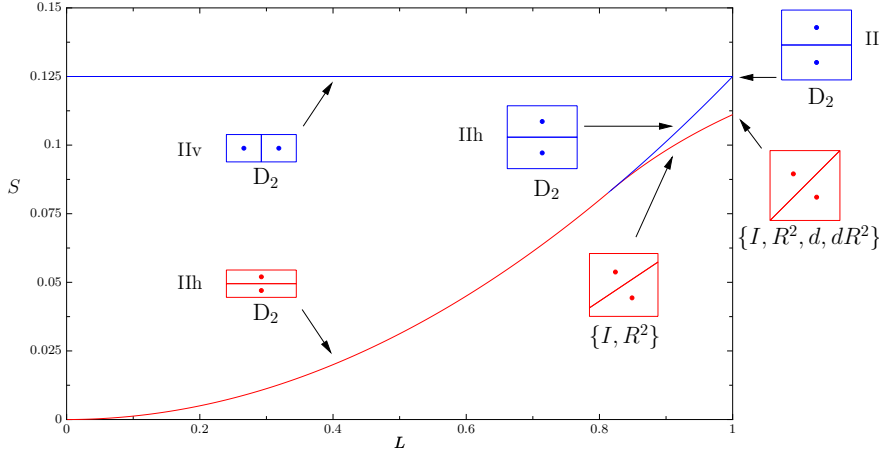


FIG. 4.1. Bifurcation diagram showing equilibrium configurations for $N = 2$ agents. In this and other bifurcation diagrams, blue (resp., red) lines/plots represent stable (resp., unstable) equilibrium configurations. Sample configurations are shown along with their isotropy subgroups.

values of the linearized evolution equations directly. The linearized equations are generated from (2.3) using numerical central differences.

As a measure of an equilibrium configuration in our bifurcation diagrams, we use

$$S = \sum_{i=1}^N [(x_i - \bar{x})^2 + (y_i - \bar{y})^2], \quad (4.1)$$

where (\bar{x}, \bar{y}) is the center of the domain D . Equilibrium configurations on the same group orbit have identical values of S , while solutions which are not related by symmetry typically have different values of S .

The possible bifurcations that occur are saddle-node bifurcations, in which two equilibrium configurations “collide” and disappear, and pitchfork bifurcations which give birth to a new branch of symmetry-related equilibria with one of the Z_2 symmetries broken, for example $D_4 \rightarrow Z_2$ or $Z_2 \rightarrow \{I\}$.

The bifurcation diagram showing equilibrium configurations for $N = 2$ agents is shown in Figure 4.1. For small values of L , the configuration with a vertical shared boundary for the Voronoi cells (which we call IIv) is stable, while the configuration with a horizontal shared boundary (which we call IIIh) is unstable. Both IIv and IIIh have D_2 symmetry. At $L = 0.817$, IIIh undergoes a pitchfork bifurcation, becoming stable for larger values of L and giving birth to a new branch of unstable solutions with isotropy subgroup $\{I, R^2\} \cong Z_2$. Consequently, the solutions IIv and IIIh are both stable for $0.817 \leq L \leq 1$. At $L = 1$, IIv and IIIh are stable, symmetry-related solutions for the square domain (see Figure 3.3). At $L = 1$, the unstable configuration acquires the additional reflection symmetries d and dR^2 . These arise because $L = 1$ is a degenerate case for a rectangular domain; in particular, these additional symmetries are not associated with a bifurcation.

The bifurcation diagram showing equilibrium configurations for $N = 3$ agents is shown in Figure 4.2. (Details of these bifurcations can be seen in Figures 4.3 and 4.4.) There are four different pitchfork bifurcations, described in the following for increasing L :

- $L = 0.469$: a configuration with isotropy subgroup $\{I, dR\} \cong Z_2$ gains stability and a branch of unstable configurations with trivial isotropy subgroup $\{I\}$ is born,
- $L = 0.627$: a configuration with isotropy subgroup $\{I, dR^3\} \cong Z_2$ loses stability and the branch of unstable configurations with trivial isotropy subgroup $\{I\}$ ceases to exist,
- $L = 0.666$: a configuration with isotropy subgroup D_2 loses stability and a branch of unstable configurations with isotropy subgroup $\{I, dR^3\} \cong Z_2$ ceases to exist,
- $L = 0.931$: a configuration with isotropy subgroup $\{I, dR^3\}$ gains stability, and a branch of unstable configurations with trivial isotropy subgroup $\{I\}$ is born.

There is also a saddle-node bifurcation at $L = 0.607$ involving solutions with isotropy subgroup $\{I, dR^3\} \cong Z_2$. Note that the unstable solutions with trivial isotropy subgroup $\{I\}$ which are born in the pitchfork bifurcation at $L = 0.931$ acquire the additional reflection symmetry d at $L = 1$; this arises from the degeneracy of the domain shape at $L = 1$. We see that several ranges of L values exist for which there are stable equilibria which are not related by symmetry.

The bifurcation diagrams showing equilibrium configurations for $N = 4$ and $N = 5$ agents are shown in Figures 4.5 and 4.6, respectively. Because of the complexity of these diagrams, we do not describe them in detail, nor do we specify the isotropy subgroups of the various equilibrium configurations. But we do note that there are ranges of L for which there are stable equilibria which are not related by symmetry.

5. Conclusion . We have analyzed the territorial model from [27], which is based on Voronoi tessellations to account for interactions between individuals in determining territories. For rectangular domains and for small population sizes, we found that there are distinct coexisting stable equilibrium configurations, including the possibility of stable equilibria that are *not* related by symmetry to each other and which represent truly distinct configurations that the population can end up in. The configuration that the population equilibrates to, and the cell in which each agent ends up, is determined by the initial positions of the agents. By considering initial positions distributed randomly on the square, we gave a statistical characterization of the likelihood of the system reaching these equilibria; this can be interpreted as a statistical characterization of the relative sizes of different basins of attraction for the equilibria. Furthermore, we found that the final territory that an agent obtains can have a wide range of areas, which suggests that an individual can obtain a competitive advantage or disadvantage due entirely to the initial positions of the agents. Finally, by treating the ratio of the length of the shorter side to the length of the longer side of the rectangle as a bifurcation parameter, we numerically explored how stable and unstable equilibrium configurations are related to each other.

Although the geometry considered here is too special to be of direct relevance to field observations, our results suggest how controlled laboratory experimentation could be used to verify or discount this particular model of territorial behavior for different species. One simply randomly positions a small number of individuals in a square or rectangular domain, and observes over multiple trials what configuration they settle down to. If the agents are effectively using the model from [27] to determine their territories, then, depending on the number of agents and the shape of the container, on some trials one would expect settling to a particular equilibrium of one type, and

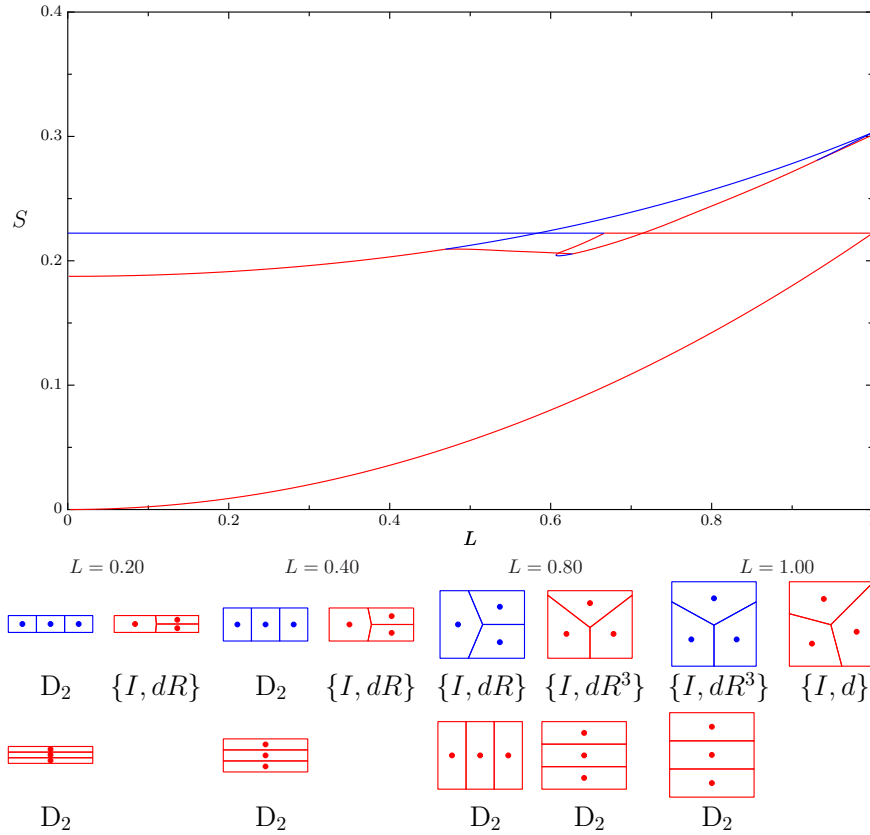


FIG. 4.2. Bifurcation diagram showing equilibrium configurations for $N = 3$ agents. For the specified values of L , the plots of the configurations are shown for decreasing S value, in the order: first row first column, first row second column, second row first column, etc. The isotropy subgroups of these configurations are indicated. More detail is shown in Figures 4.3 and 4.4.

in others settling to an equilibrium of another non-symmetry-related type.

The presence of coexisting stable equilibria also suggests that noise-induced transitions between different states might occur. Such transitions have recently been identified for biological systems for the switching between symmetry-related clockwise and counterclockwise motions for marching locusts constrained to a ring [6], and switching between qualitatively different collective motion states [24].

REFERENCES

- [1] Adams, E. S., 2001. Approaches to the study of territory size and shape. *Annu. Rev. Ecol. Syst.* 32, 277-303.
- [2] Barlow, G. W., 1974. Hexagonal territories. *Anim. Behav.* 22, 876-878.
- [3] Buckley, P. A., Buckley, F. G., 1977. Hexagonal packing of Royal Tern nests. *Auk*. 94, 36-43.
- [4] Clayton, D. A., Vaughan, T. C., 1982. Pentagonal territories of the mudskipper *Boleophthalmus boddarti* (Pisces: Gobiidae). *Copeia* 1, 233-235.
- [5] Clayton, D. A., Wright, J. M., 1989. Mud-walled territories and feeding behaviour of *Boleophthalmus boddarti* (Pisces: Gobiidae) on the mudflats of Kuwait. *J. Ethol.* 7, 91-95.
- [6] Buhl, J., Sumpter, D. J. T., Couzin, I. D., Hale, J. J., Despland, E., Miller, E. R., Simpson, S.

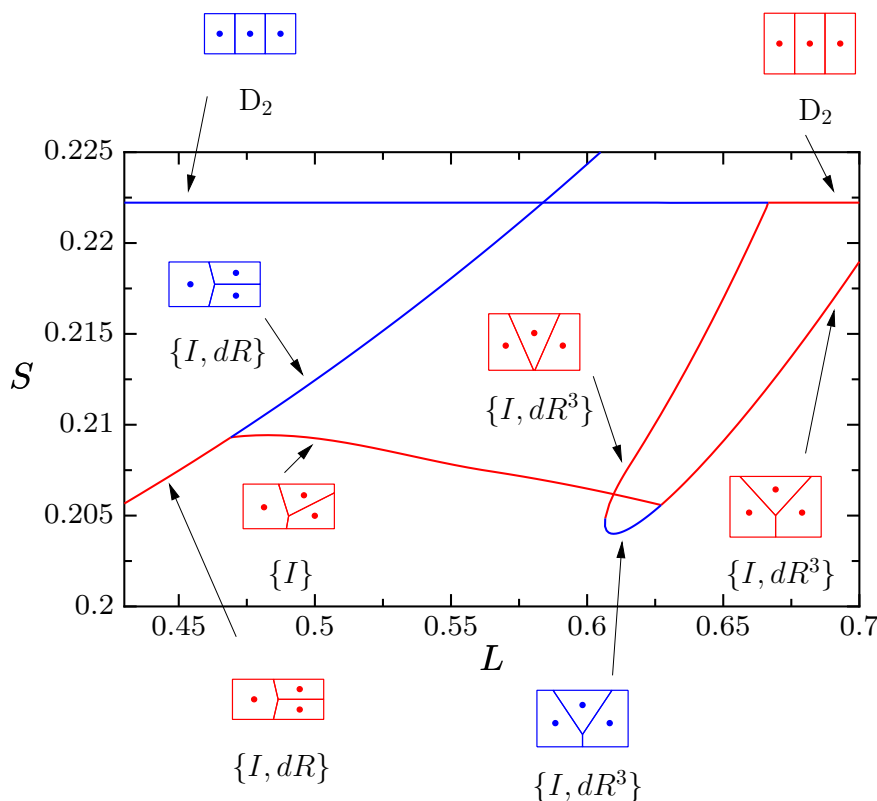


FIG. 4.3. Details of the bifurcation diagram shown in Figure 4.2.

- J., 2006. From disorder to order in marching locusts. *Science*. 312, 1402-1406.
- [7] Burkhardt, J. http://www.scs.fsu.edu/~burkhardt/m_src/geometry/geometry.html
- [8] Chossat, P., Lauterbach, R., 2000. *Methods in Equivariant Bifurcations and Dynamical Systems*. World Scientific, Singapore.
- [9] Cortés, J., Martínez, S., Karatas, T., and Bullo, F., 2004. Coverage control for mobile sensing networks. *IEEE Trans. Robotics and Automation*, 20, 243-255.
- [10] Dhooge, A., Govaerts, W., Kuznetsov, Y.A., Mestrom, W., Riet, A.M., Sautois, B., 2006. MATCONT and CL-MATCONT: Continuation toolboxes in Matlab. <http://www.matcont.ugent.be/>.
- [11] Doedel, E.J., Keller, H.B., Kernevez, J.P., 1991. Numerical analysis and control of bifurcation problems, part I. *Int. J. Bif. Chaos*. 1, 493-520.
- [12] Doedel, E.J., Keller, H.B., Kernevez, J.P., 1991. Numerical analysis and control of bifurcation problems, part II. *Int. J. Bif. Chaos*. 1, 745-772.
- [13] Doedel, E.J., Champneys, A.R., Fairgrieve, T.F., Kuznetsov, Y.A., Sandstede, B., Wang, X., 1998. AUTO 97: continuation and bifurcation software for ordinary differential equations. <http://indy.cs.concordia.ca/auto/>.
- [14] Doncaster, C. P., Woodroffe, R., 1993. Den site can determine shape and size of badger territories: implications for group-living. *Oikos* 66, 88-93.
- [15] Du, Q., Faber, V., Gunzburger, M., 1999. Centroidal Voronoi tessellations: applications and algorithms. *SIAM Review* 41, 637-676.
- [16] Golubitsky, M., Stewart, I., Schaeffer, D. G., 1988. *Singularities and Groups in Bifurcation Theory, Vol. 2*. Springer, New York.
- [17] Golubitsky, M. and Stewart, I., 2002. *The Symmetry Perspective*. Birkhauser Verlag, Basel.
- [18] Grant, P. R., 1968. Polyhedral territories of animals. *Amer. Naturalist* 102, 75-80.
- [19] Hasegawa, M., Tanemura, M., 1976. On the pattern of space division by territories. *Ann. Inst.*

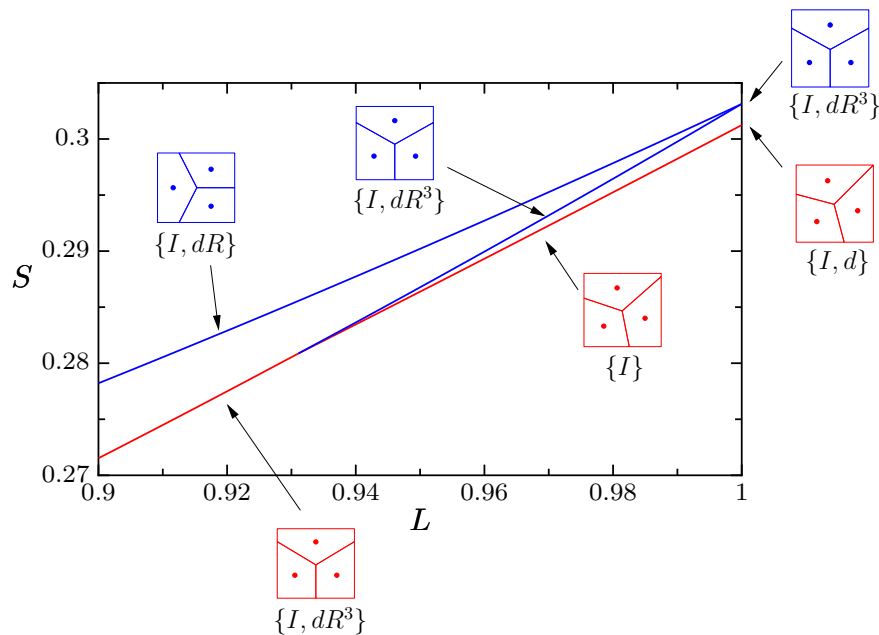


FIG. 4.4. Details of the bifurcation diagram shown in Figure 4.2.

- Statist. Math. 28, 509-519.
- [20] Hasegawa, M., Tanemura, M., 1980. Spatial patterns of territories, in: Matusita, K. (Ed.), Recent Developments in Statistical Inference and Data Analysis, North-Holland, Amsterdam, pp. 73-78.
- [21] Honda, H., 1978. Description of cellular patterns by Dirichlet domains: the two-dimensional case. *J. theor. Biol.* 72, 523-543.
- [22] Hoyle, R. B., *Pattern Formation: An Introduction to Methods*. Cambridge University Press, Cambridge.
- [23] Hsieh, C. H., Chuang, Y.-L., Huang, Y., Leung, K. K., Bertozzi, A. L., Frazzoli, E., 2006. An economical micro-car testbed for validation of cooperative control strategies, in Proc. 2006 American Control Conference, Minneapolis, Minnesota, pp. 1446-1451.
- [24] Kolpas, A., Moehlis, J., Kevrekidis, I. G., 2007. Stochasticity-induced switching between collective motion states. *Proc. Nat. Acad. Sci. USA* 104, 5931-5935.
- [25] Lomont, J. S., 1993. *Applications of Finite Groups*. Dover, New York.
- [26] Moehlis, J. and Knobloch, E., 2007. Equivariant Dynamical Systems, Scholarpedia: http://www.scholarpedia.org/article/Equivariant_Dynamical_Systems
- [27] Tanemura, M., Hasegawa, M., 1980. Geometrical models of territory. I. Models for synchronous and asynchronous settlement of territories. *J. theor. Biol.* 82, 477-496.
- [28] Wilson, E. O., 1975. *Sociobiology: The New Synthesis*. Harvard Univ. Press, Cambridge.

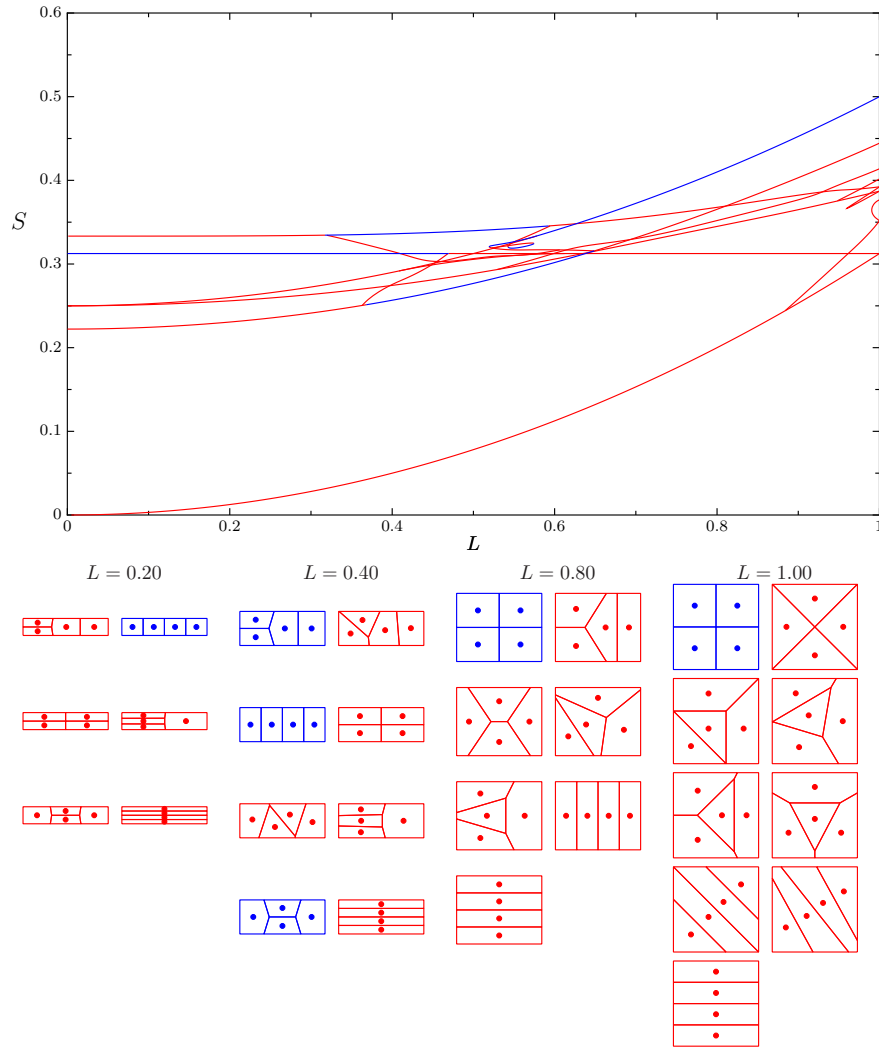


FIG. 4.5. Bifurcation diagram showing equilibrium configurations for $N = 4$ agents. For the specified values of L , the plots of the configurations are shown for decreasing S value, in the order as explained in the caption of Figure 4.2.

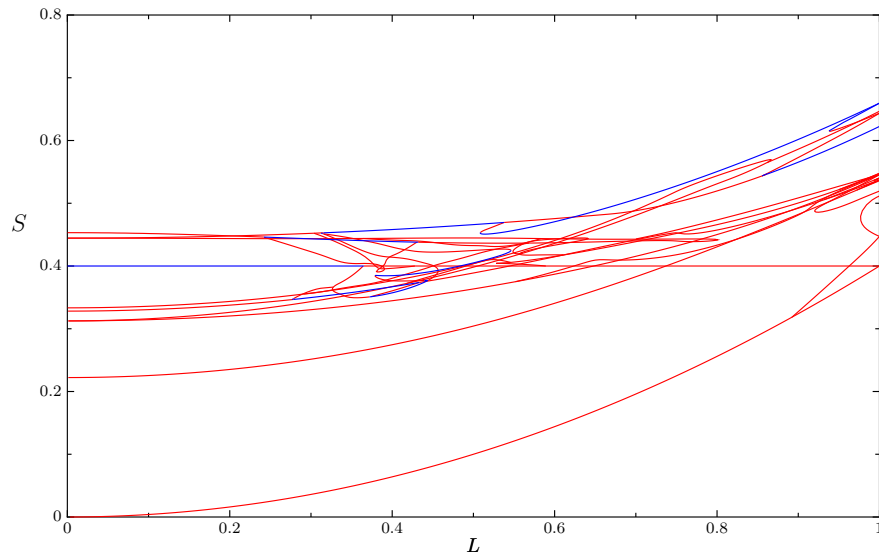


FIG. 4.6. Bifurcation diagram showing equilibrium configurations for $N = 5$ agents. Corresponding equilibrium configurations are shown in Figure 4.7.

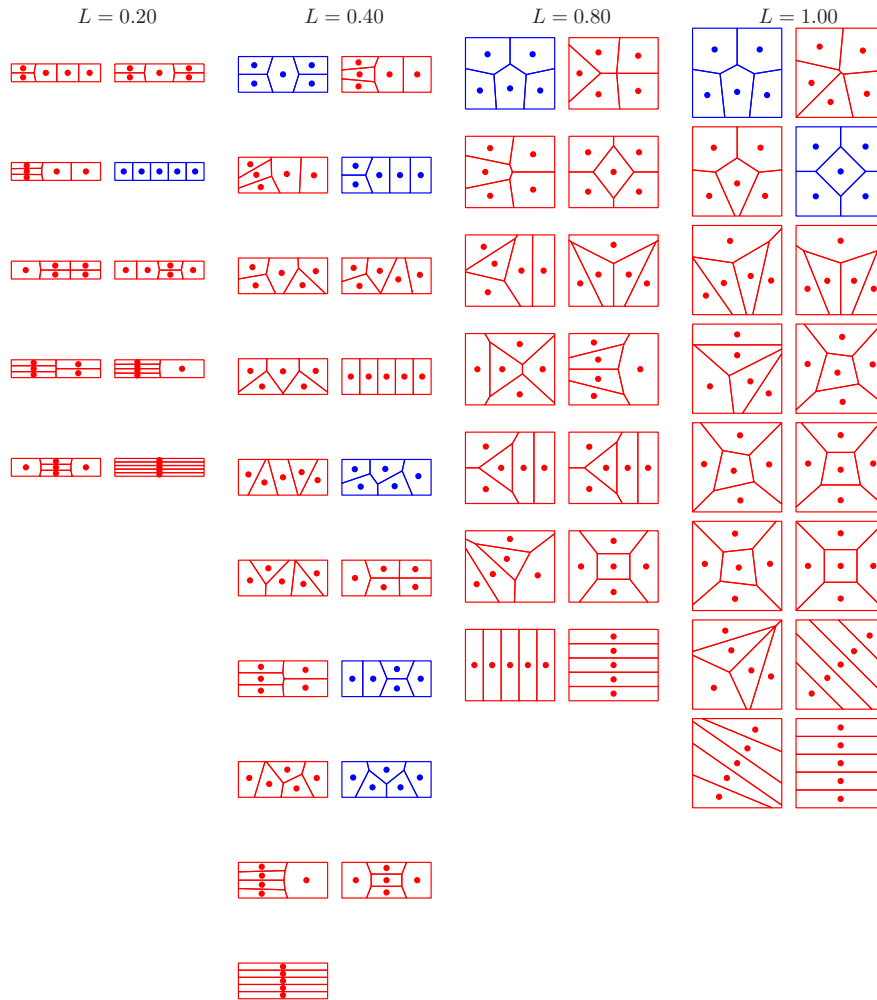


FIG. 4.7. *Equilibrium configurations for $N = 5$ agents. For the specified values of L , the plots of the configurations are shown for decreasing S value according to Figure 4.6, in the order as explained in the caption of Figure 4.2.*